ISOGEOMETRIC BDDC PRECONDITIONERS
WITH DELUXE SCALING[*]

L. BEIRÃO DA VEIGA[†], L. F. PAVARINO[†], S. SCACCHI[†], O. B. WIDLUND[‡], AND
S. ZAMPINI[§]

Abstract. A balancing domain decomposition by constraints (BDDC) preconditioner with a novel scaling, introduced by Dohrmann for problems with more than one variable coefficient and here denoted as deluxe scaling, is extended to isogeometric analysis of scalar elliptic problems. This new scaling turns out to be more powerful than the standard ρ- and stiffness scalings considered in a previous isogeometric BDDC study. Our h-analysis shows that the condition number of the resulting deluxe BDDC preconditioner is scalable with a quasi-optimal polylogarithmic bound which is also independent of coefficient discontinuities across subdomain interfaces. Extensive numerical experiments support the theory and show that the deluxe scaling yields a remarkable improvement over the older scalings, in particular for large isogeometric polynomial degree and high regularity.

Key words. domain decomposition, BDDC preconditioners, isogeometric analysis, elliptic problems

AMS subject classifications. 65F08, 65N30, 65N35, 65N55

DOI. 10.1137/130917399

1. Introduction. The design of efficient and scalable iterative solvers for isogeometric analysis (IGA) (see, e.g., the initial papers [21, 2], the book [12], or the mathematical review paper [3]) is far from routine due to the integration of finite element analysis and computer aided design techniques which are required to build smooth and high-order discretizations based on nonuniform rational B-splines (NURBS) representations for both the domain geometry and finite element basis functions. In particular, there are challenges arising from the fact that the basis functions are not nodal and can have wider support than finite element basis functions, properties that lead to stiffness matrices that are (for a fixed mesh) smaller but less sparse than in the finite element case. Moreover, whenever the Schur complement system associated to some subdomain subdivision is considered, the large support of the basis functions yields a wider (fat) interface in the index space.

The main goal of this paper is to design, analyze, and test a balancing domain decomposition by constraints (BDDC) (see [15, 31]) preconditioner for IGA based on a novel type of interface averaging, which we will denote by *deluxe scaling*. This variant was recently introduced by Dohrmann and Widlund in a study of $H(curl)$ problems; see [17] and also [34] for its application to problems in $H(div)$ and [27] for Reissner–Mindlin plates. In our previous work on isogeometric BDDC [6], standard

BDDC scalings were employed with weights for the averaging built directly from the values of the elliptic coefficients in each subdomain (ρ-scaling) or from the values of the diagonal elements of local and global stiffness matrices (stiffness scaling). The novel deluxe scaling, originally developed to deal with elliptic problems with more than one variable coefficient, is instead based on solving local problems built from local Schur complements associated with sets of what are known as the dual variables. This new scaling turns out to be much more powerful than the standard ρ- and stiffness scaling even for scalar elliptic problems with one variable coefficient. The main result of our h-analysis shows that the condition number of the resulting deluxe BDDC preconditioner satisfies the same quasi-optimal polylogarithmic bound in the ratio H/h of subdomain to element diameters, as in [6], and that it is independent of the number of subdomains and jumps of the coefficients of the elliptic problem across subdomain interfaces. Moreover, our numerical experiments with deluxe scaling show a remarkable improvement, in particular, for increasing polynomial degree p of the isogeometric elements, regardless of the element regularity κ. In particular, for two-dimensional (2D) problems, the convergence rate of deluxe BDDC appears to be independent of p, while for three-dimensional (3D) problems, it depends only mildly on p and provides results which are several orders of magnitude better than what has been obtained with stiffness and ρ-scaling.

Recent work on IGA preconditioners have focused on overlapping Schwarz preconditioners [5, 7, 9], multigrid methods [19], and nonoverlapping preconditioners [6, 24]. Other works have focused on isogeometric mortar discretizations [20] and the computational costs of isogeometric iterative solvers [11]. Among the recent extensions of BDDC methods, we mention the work on mortar discretizations [22, 23], discontinuous Galerkin methods [14], advection-diffusion and indefinite problems [38, 30], inexact solvers [16, 29], Reissner–Mindlin plates [4, 26], spectral elements [35], and multilevel algorithms [37, 33].

We remark that we could also consider finite element tearing and interconnecting–dual primal (FETI-DP) algorithms (see, e.g., [18, 25]), defined with the same set of primal constraints as our BDDC algorithm, since it is known that then the BDDC and FETI-DP operators have the same eigenvalues with the exception of at most two; see [32, 28, 10].

The rest of this paper is organized as follows. We recall the basics on IGA discretizations of elliptic problems in section 2. In section 3, we introduce the domain and space decompositions in the isogeometric context, the required restriction and interpolation operators, and the deluxe scaling, and we construct the BDDC preconditioner. In section 4, we prove a condition number bound for the deluxe BDDC preconditioned operator. In section 5, the results of serial and parallel numerical tests in two and three dimensions are presented, confirming our theoretical estimates.

2. Isogeometric discretization of scalar elliptic problems. We consider the model elliptic problem on a bounded and connected CAD domain $\Omega \subset \mathbb{R}^d$, $d = 2, 3$,

$$(2.1) \qquad -\nabla \cdot (\rho \nabla u) = f \text{ in } \Omega, \quad u = 0 \text{ on } \partial\Omega,$$

where ρ is a scalar field satisfying $0 < \rho_{min} \le \rho(x) \le \rho_{max}$ for all $x \in \Omega$.

We discretize (2.1) with IGA based on B-splines and NURBS basis functions; see, e.g., [12]. When we describe our problem and the iterative method, we will confine our discussion, for simplicity, mostly to the 2D single-patch case, but we will also comment on extensions to three dimensions and multipatch domains.

The bivariate B-spline discrete space is defined by

$$(2.2) \qquad \widehat{\mathcal{S}}_h := \operatorname{span}\{B_{i,j}^{p,q}(\xi,\eta),\ i=1,\dots,n,\, j=1,\dots,m\},$$

where the bivariate B-spline basis functions $B_{i,j}^{p,q}(\xi,\eta) = N_i^p(\xi)\,M_j^q(\eta)$ are defined by tensor products of one-dimensional B-splines functions $N_i^p(\xi)$ and $M_j^q(\eta)$ of degree p and q, respectively (in our numerical experiments, we will consider only the case of $p = q$). Analogously, the NURBS space is the span of NURBS basis functions defined in one dimension by

$$(2.3) \qquad R_i^p(\xi) := \frac{N_i^p(\xi)\omega_i}{\sum_{\hat{\imath}=1}^n N_{\hat{\imath}}^p(\xi)\omega_{\hat{\imath}}} = \frac{N_i^p(\xi)\omega_i}{w(\xi)},$$

with the weight function $w(\xi) := \sum_{\hat{\imath}=1}^n N_{\hat{\imath}}^p(\xi)\omega_{\hat{\imath}} \in \widehat{\mathcal{S}}_h$, and in two dimensions by a tensor product

$$(2.4) \qquad R_{i,j}^{p,q}(\xi,\eta) := \frac{B_{i,j}^{p,q}(\xi,\eta)\omega_{i,j}}{\sum_{\hat{\imath}=1}^n \sum_{\hat{\jmath}=1}^m B_{\hat{\imath},\hat{\jmath}}^{p,q}(\xi,\eta)\omega_{\hat{\imath},\hat{\jmath}}} = \frac{B_{i,j}^{p,q}(\xi,\eta)\omega_{i,j}}{w(\xi,\eta)},$$

where $w(\xi,\eta)$ is the weight function and $\omega_{i,j} = (\mathbf{C}_{i,j}^\omega)_3$ the positive weights associated with an $n \times m$ net of control points $\mathbf{C}_{i,j}$. The discrete space of NURBS functions on the domain Ω is defined as the span of the *push-forward* of the NURBS basis functions (2.4) (see, e.g., [21, 12])

$$(2.5) \qquad \mathcal{N}_h := \operatorname{span}\{R_{i,j}^{p,q} \circ \mathbf{F}^{-1},\ \text{with } i=1,\dots,n;\, j=1,\dots,m\},$$

with $\mathbf{F} : \widehat{\Omega} \to \Omega$, the geometrical map between parameter and physical spaces

$$(2.6) \qquad \mathbf{F}(\xi,\eta) = \sum_{i=1}^n \sum_{j=1}^m R_{i,j}^{p,q}(\xi,\eta)\mathbf{C}_{i,j}.$$

For simplicity, we will consider the case with a Dirichlet boundary condition imposed on all of $\partial\Omega$ and can then define the spline space in the parameter space by

$$\widehat{V}_h := [\widehat{\mathcal{S}}_h \cap H_0^1(\widehat{\Omega})]^2 = [\operatorname{span}\{B_{i,j}^{p,q}(\xi,\eta),\ i=2,\dots,n-1,\, j=2,\dots,m-1\}]^2$$

and the NURBS space in physical space by

$$U_h := [\mathcal{N}_h \cap H_0^1(\Omega)]^2 = [\operatorname{span}\{R_{i,j}^{p,q} \circ \mathbf{F}^{-1},\ \text{with } i=2,\dots,n-1;\, j=2,\dots,m-1\}]^2.$$

The IGA formulation of problem (2.1) then reads

$$(2.7) \qquad \begin{cases} \text{Find } u_h \in U_h \text{ such that} \\ a(u_h,v_h) = \langle f, v_h \rangle \qquad \forall v \in U_h, \end{cases}$$

with the bilinear form $a(u_h,v_h) = \int_\Omega \rho \nabla u_h \nabla v_h\, dx$ and the right-hand side $\langle f, v_h \rangle = \int_\Omega f v_h\, dx$.

3. BDDC preconditioners for the Schur complement system. When using iterative substructuring methods, such as BDDC, we first reduce the problem to one on the interface by implicitly eliminating the interior degrees of freedom, a process known as static condensation; see, e.g., Toselli and Widlund [36, Ch. 4].

3.1. Knots and subdomain decomposition. A decomposition is first built for the underlying space of spline functions in the parametric space and is then easily extended to the NURBS space in the physical domain. From the full set of knots, $\{\xi_1 = 0, \ldots, \xi_{n+p+1} = 1\}$, we select a subset

$$0 = \xi_{i_1} < \xi_{i_2} < \cdots < \xi_{i_N} < \xi_{i_{N+1}} = 1$$

of nonrepeated knots. The interface knots are given by ξ_{i_k} for $k = 2, \ldots, N$, and they define a decomposition of the closure of the reference interval into subdomains

$$\overline{(\widehat{I})} = [0,1] = \overline{\Big(\bigcup_{k=1,\ldots,N} \widehat{I}_k \Big)}, \quad \text{with} \quad \widehat{I}_k = (\xi_{i_k}, \xi_{i_{k+1}}),$$

that we assume to have similar lengths $H_k := \text{diam}(\widehat{I}_k) \approx H$. In more dimensions, we just use tensor products. Thus, in two dimensions, we define the subdomains by

$$(3.1) \quad \widehat{I}_k = (\xi_{i_k}, \xi_{i_{k+1}}), \quad \widehat{I}_l = (\eta_{j_l}, \eta_{j_{l+1}}), \quad \widehat{\Omega}_{kl} = \widehat{I}_k \times \widehat{I}_l, \quad 1 \le k \le N_1, \ 1 \le l \le N_2.$$

For simplicity, we reindex the subdomains using only one index to obtain the decomposition of our domain

$$\overline{\widehat{\Omega}} = \bigcup_{k=1,\ldots,K} \overline{\widehat{\Omega}}_k$$

into $K = N_1 N_2$ subdomains, and, analogously, into $K = N_1 N_2 N_3$ subdomains in three dimensions. Throughout this paper, we assume that both the subdomains and elements defined by the coarse and full sets of knot vectors are *shape regular* and with quasi-uniform characteristic diameters H and h, respectively.

3.2. The Schur complement system. As in classical iterative substructuring, we reduce the problem to one on the interface

$$(3.2) \quad \Gamma := \Big(\bigcup_{k=1}^{K} \partial \widehat{\Omega}_k \Big) \backslash \partial \widehat{\Omega}$$

by static condensation, i.e., by eliminating the interior degrees of freedom associated with the basis functions with support in each subdomain. The resulting Schur complement for $\widehat{\Omega}_k$ and its local interface $\Gamma_k := \partial \widehat{\Omega}_k \setminus \partial \widehat{\Omega}$ will be denoted by $S^{(k)}$.

In what follows, we will use the following sets of indices:

$$\Theta_\Omega = \{(i,j) \in \mathbb{N}^2 : \ 2 \le i \le n-1, 2 \le j \le m-1\},$$
$$\Theta_\Gamma = \{(i,j) \in \Theta_\Omega : \ \text{supp}(B_{i,j}^{p,q}) \cap \Gamma \ne \emptyset\}.$$

We note that Θ_Γ consists of indices associated with a "fat" interface that typically consists of several layers of knots associated with the basis functions with support intersecting two or more subdomains; see, e.g., Figure 1. Later we will split this fat interface into fat vertices and edges (and faces in three dimensions). The discrete interface and local spaces are defined as

$$(3.3) \quad \widehat{V}_\Gamma := \text{span}\{B_{i,j}^{p,q}, (i,j) \in \Theta_\Gamma\}, \qquad V_I^{(k)} := \widehat{V}_h \cap H_0^1(\widehat{\Omega}_k).$$

The space $\widehat{V}_h$ can be decomposed as

$$(3.4) \qquad \oplus_{k=1}^K V_I^{(k)} + \mathcal{H}(\widehat{V}_\Gamma),$$

where $\mathcal{H} : \widehat{V}_\Gamma \to \widehat{V}_h$, is the piecewise discrete spline harmonic extension operator, which provides the minimal energy extension of values given in $\widehat{V}_\Gamma$.

The interface component of the discrete solution satisfies the reduced system

$$(3.5) \qquad s(u_\Gamma, v_\Gamma) = \langle \widehat{f}, v_\Gamma \rangle \quad \forall v_\Gamma \in \widehat{V}_\Gamma,$$

with a suitable right-hand side $\widehat{f}$ and a Schur complement bilinear form defined by

$$(3.6) \qquad s(w_\Gamma, v_\Gamma) := a(\mathcal{H}(w_\Gamma), \mathcal{H}(v_\Gamma)).$$

For simplicity, in what follows, we will drop the subscript Γ for functions in $\widehat{V}_\Gamma$.

In matrix form, (3.5) is the Schur complement system

$$(3.7) \qquad \widehat{S}_\Gamma w = \widehat{f},$$

where $\widehat{S}_\Gamma = A_{\Gamma\Gamma} - A_{\Gamma I} A_{II}^{-1} A_{\Gamma I}^T$, $\widehat{f} = f_\Gamma - A_{\Gamma I} A_{II}^{-1} f_I$ are obtained from the original discrete problem by Gaussian elimination after reordering the spline basis functions into sets of interior (subscript I) and interface (subscript Γ) basis functions

$$(3.8) \qquad \begin{pmatrix} A_{II} & A_{\Gamma I}^T \\ A_{\Gamma I} & A_{\Gamma\Gamma} \end{pmatrix} \begin{pmatrix} w_I \\ w_\Gamma \end{pmatrix} = \begin{pmatrix} f_I \\ f_\Gamma \end{pmatrix}.$$

The Schur complement system (3.7) is solved by a preconditioned conjugate gradient (PCG) iteration, where $\widehat{S}_\Gamma$ is never explicitly formed since the action of $\widehat{S}_\Gamma$ on a vector is computed by solving Dirichlet problems for individual subdomains and some sparse matrix-vector multiplications, which are also needed when working with the local Schur complements required by the application of the BDDC preconditioner defined below. The preconditioned Schur complement system solved by PCG is then

$$(3.9) \qquad M_{\mathrm{BDDC}}^{-1} \widehat{S}_\Gamma w = M_{\mathrm{BDDC}}^{-1} \widehat{f},$$

where M_{BDDC}^{-1} is the BDDC preconditioner, defined in (3.15) below using some restriction and scaling operators associated with the following subspace decompositions.

3.3. Subspace decompositions. Analogously to the space splitting (3.4), we split the local space $V^{(k)}$ defined in (3.3) into a direct sum of its interior (I) and interface (Γ) subspaces $V^{(k)} = V_I^{(k)} \bigoplus V_\Gamma^{(k)}$, where

$$V_I^{(k)} := \mathrm{span}\{B_{i,j}^{p,q}, (i,j) \in \Theta_I^{(k)}\}, \ \Theta_I^{(k)} := \{(i,j) \in \Theta_\Omega : \ \mathrm{supp}(B_{i,j}^{p,q}) \subset \widehat{\Omega}_k\},$$

$$V_\Gamma^{(k)} := \mathrm{span}\{B_{i,j}^{p,q}, (i,j) \in \Theta_\Gamma^{(k)}\}, \ \Theta_\Gamma^{(k)} := \{(i,j) \in \Theta_\Gamma : \ \mathrm{supp}(B_{i,j}^{p,q}) \cap (\partial\widehat{\Omega}_k \cap \Gamma_k) \neq \emptyset\},$$

and we define the associated product spaces by

$$V_I := \prod_{k=1}^K V_I^{(k)}, \quad V_\Gamma := \prod_{k=1}^K V_\Gamma^{(k)}.$$

The functions in V_Γ are generally discontinuous (multivalued) across Γ, while our isogeometric approximations belong to $\widehat{V}_\Gamma$, the subspace of V_Γ of functions continuous
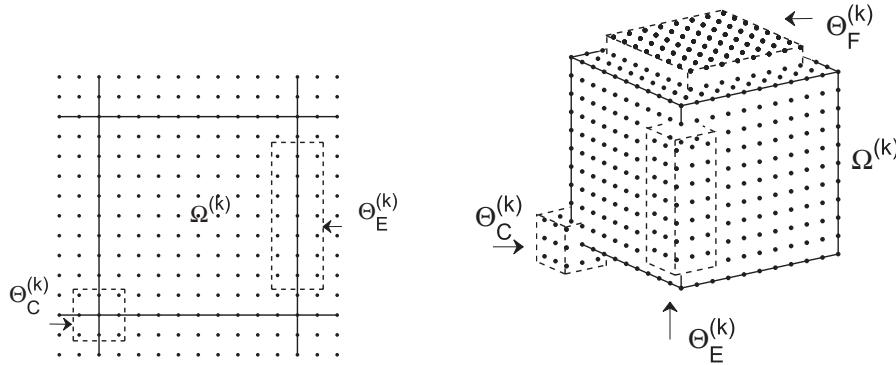
FIG. 1. *Index space schematic illustration of interface equivalence classes for a subdomain $\Omega^{(k)}$ in two dimensions (left) and three dimensions (right) in parametric space, with $p = 3, \kappa = 2$: examples of a fat vertex $\Theta_C^{(k)}$, consisting of $(\kappa + 1)^2$ knots in two dimensions and $(\kappa + 1)^3$ in three dimensions, fat edge $\Theta_E^{(k)}$, consisting of $(\kappa + 1)$ "slim" edges in two dimensions and $(\kappa + 1)^2$ in three dimensions, fat face $\Theta_F^{(k)}$, consisting of $\kappa + 1$ slim faces in three dimensions.*

(single-valued) across Γ. We will select some interface basis functions as *primal* (subscript Π), that will be made continuous across the interface and will be subassembled between their supporting elements, and we will call *dual* (subscript Δ) the remaining interface degrees of freedom that can be discontinuous across the interface and which vanish at the primal degrees of freedom. This splitting allows us to decompose each local interface space into primal and dual subspaces $V_\Gamma^{(k)} = V_\Pi^{(k)} \bigoplus V_\Delta^{(k)}$, and we can define the associated product spaces by

$$V_\Delta := \prod_{k=1}^{K} V_\Delta^{(k)}, \quad V_\Pi := \prod_{k=1}^{K} V_\Pi^{(k)}.$$

We also need an intermediate subspace $\widetilde{V}_\Gamma \subset V_\Gamma$ of partially continuous basis functions

$$\widetilde{V}_\Gamma := V_\Delta \bigoplus \widehat{V}_\Pi,$$

where the product space V_Δ has been defined above and $\widehat{V}_\Pi$ is a global subspace of the selected primal variables. Particular choices of primal sets are given in section 3.4 below.

In order to define our preconditioners, we will need the following restriction and interpolation operators represented by matrices with elements in the set $\{0, 1\}$:

$$(3.10) \quad \begin{array}{lll} \widetilde{R}_{\Gamma\Delta} : \widetilde{V}_\Gamma \longrightarrow V_\Delta, & \widetilde{R}_{\Gamma\Pi} : \widetilde{V}_\Gamma \longrightarrow \widehat{V}_\Pi, & \widehat{R}_\Pi : \widehat{V}_\Gamma \longrightarrow \widehat{V}_\Pi, \\ R_\Delta^{(k)} : V_\Delta \longrightarrow V_\Delta^{(k)}, & R_\Pi^{(k)} : \widehat{V}_\Pi \longrightarrow \widehat{V}_\Pi^{(k)}, & \widehat{R}_\Delta^{(k)} : \widehat{V}_\Gamma \longrightarrow V_\Delta^{(k)}. \end{array}$$

For any edge/face $\mathcal{F}$, we also define $R_\mathcal{F}$ as the restriction matrix to $\mathcal{F}$.

3.4. Choice of primal constraints. The choice of primal degrees of freedom is fundamental for the construction of efficient BDDC preconditioners. In three dimensions, we split the interface Γ (see 3.2) into certain equivalence classes, associated with subdomain vertices (C), edges (E), and faces (F), defined by the set of indices of

the subdomains the boundaries of which the degrees of freedom belong to. We define the following index sets associated with fat vertices, edges, and faces (and their local versions $\Theta_C^{(k)}, \Theta_E^{(k)}, \Theta_F^{(k)}$ associated with a generic subdomain $\Omega^{(k)}$; see Figure 1):

$$\Theta_C = \{(i,j,k) \in \Theta_\Gamma : \operatorname{supp}(B_{i,j,k}^{p,q;r}) \cap C \neq \emptyset\},$$
$$\Theta_E = \{(i,j,k) \in \Theta_\Gamma / \Theta_C : \operatorname{supp}(B_{i,j,k}^{p,q;r}) \cap E \neq \emptyset\},$$
$$\Theta_F = \{(i,j,k) \in \Theta_\Gamma / (\Theta_C \cup \Theta_E) : \operatorname{supp}(B_{i,j,k}^{p,q;r}) \cap F \neq \emptyset\}.$$

We consider the following three choices of primal variables (the last is used only in the 3D case).

(i) $\widehat{V}_\Pi = \widehat{V}_\Pi^C$ is the set of vertex basis functions with indices belonging to Θ_C. This choice is not always sufficient to obtain scalable and fast preconditioners, in particular for problems in three dimensions, and this has motivated the search for richer primal sets that may yield faster rates of convergence.

(ii) $\widehat{V}_\Pi = \widehat{V}_\Pi^{C+E}$ is the previous set augmented with the subdomain edge averages, each computed over the knots of a fat edge $\mathcal{E} \in \Theta_E$. We can also decompose the fat edge $\mathcal{E}$ into (p in two dimensions or p^2 in three dimensions) slim edges parallel to the subdomain edge and use the edge average for each such edge as a primal variable.

(iii) $\widehat{V}_\Pi = \widehat{V}_\Pi^{C+E+F}$ is the previous set augmented with the subdomain face averages, each computed over the knots of a fat face $\mathcal{F} \in \Theta_F$. We can also decompose the fat face $\mathcal{F}$ into p slim faces parallel to the subdomain face and use a face average for each such face as a primal variable.

When working with the primal sets $\widehat{V}_\Pi^{C+E}$ and $\widehat{V}_\Pi^{C+E+F}$ employing edge and/or face averages, we will assume that, after a change of basis, each primal variable corresponds to an explicit degree of freedom; see [28] and section 5 for implementation details. Our theoretical analysis in section 4 will focus on the simplest primal set $\widehat{V}_\Pi^C$ in two dimensions, but in our numerical experiments we will also study the two other richer choices in three dimensions.

3.5. Deluxe scaling (see Dohrmann and Widlund [17]). Let Ω_k be any subdomain in the partition, $k = 1, 2, \ldots, K$. We will indicate by Ξ_k the index set of all the Ω_j, $j \neq k$, that share an edge $\mathcal{F}$ with Ω_k. For regular quadrilateral subdomain partitions in two dimensions, the cardinality of Ξ_k is 4 (or less for boundary subdomains).

In BDDC, the average $\bar{w} := E_D w$ of an element in $w \in \widetilde{V}_\Gamma$ is computed separately for the sets of interface degrees of freedom of edge and face equivalence classes.

We define the deluxe scaling for the class of $\mathcal{F}$ with only two elements, k, j, as for an edge in two dimensions or a face in three dimensions; see subsection 4.2 for cases of equivalence classes of dual unknowns associated with more than two subdomains. We define two principal minors, $S_{\mathcal{F}}^{(k)}$ and $S_{\mathcal{F}}^{(j)}$, obtained from $S^{(k)}$ and $S^{(j)}$ by removing all rows and columns which do not belong to the degrees of freedom which are common to the (fat) boundaries of Ω_k and Ω_j.

Let $w_{\mathcal{F}}^{(k)} := R_{\mathcal{F}} w^{(k)}$; the deluxe average across $\mathcal{F}$ is then defined as

(3.11)
$$\bar{w}_{\mathcal{F}} = \left(S_{\mathcal{F}}^{(k)} + S_{\mathcal{F}}^{(j)}\right)^{-1} \left(S_{\mathcal{F}}^{(k)} w_{\mathcal{F}}^{(k)} + S_{\mathcal{F}}^{(j)} w_{\mathcal{F}}^{(j)}\right).$$

If the Schur complements of an equivalence class have small dimensions, they can be computed explicitly; otherwise the action of $(S_{\mathcal{F}}^{(k)} + S_{\mathcal{F}}^{(j)})^{-1}$ can be computed by solving a Dirichlet problem on the union of the relevant subdomains with a zero right-

hand side in the interiors of the subdomains. See the implementation details in section 5 and also Remark 3.1 at the end of this section.

Each of the relevant equivalence classes, which involve the subdomain Ω_k, will contribute to the values of $\bar{w}$. Each of these contributions will belong to $\widehat{V}_\Gamma$, after being extended by zero to $\Gamma \setminus \mathcal{F}$; the resulting element is given by $R_\mathcal{F}^T \bar{w}_\mathcal{F}$. We then add the contributions from the different equivalence classes to obtain

$$(3.12) \qquad \bar{w} = E_D w = w_\Pi + \sum_\mathcal{F} R_\mathcal{F}^T \bar{w}_\mathcal{F}.$$

E_D is a projection, and its complementary projection is given by

$$(3.13) \qquad P_D w := (I - E_D)w := P_D w = w_\Delta - \sum_\mathcal{F} R_\mathcal{F}^T \bar{w}_\mathcal{F}.$$

We remark that, with a small abuse of notation, we will, in what follows, consider $E_D w \in \widehat{V}_\Gamma$ also as an element of $\widetilde{V}_\Gamma$, by the obvious embedding $\widehat{V}_\Gamma \subset \widetilde{V}_\Gamma$. In order to rewrite E_D in matrix form, for each subdomain Ω_k, we define the scaling matrix

$$D^{(k)} = \begin{bmatrix} D_{\mathcal{F}j_1}^{(k)} & & & \\ & D_{\mathcal{F}j_2}^{(k)} & & \\ & & \ddots & \\ & & & D_{\mathcal{F}j_k}^{(k)} \end{bmatrix},$$

where $j_1, j_2, \ldots, j_k \in \Xi_k$, and the diagonal blocks are given by the deluxe scaling $D_\mathcal{F}^{(k)} := (S_\mathcal{F}^{(k)} + S_\mathcal{F}^{(j)})^{-1} S_\mathcal{F}^{(k)}$, with $\mathcal{F}$ a 2D edge or 3D face of the class associated with the subdomains Ω_k and Ω_j. For equivalence classes with more than two subdomains, see section 4.2.

We can now define the scaled local operators by $R_{D,\Gamma}^{(k)} := D^{(k)} R_\Gamma^{(k)}$, $\widetilde{R}_{D,\Delta}^{(k)} := R_{\Gamma,\Delta}^{(k)} R_{D,\Gamma}^{(k)}$ and the global scaled operator

$$(3.14) \qquad \widetilde{R}_{D,\Gamma} := \text{ the direct sum } \widehat{R}_\Pi \oplus_{k=1}^K \widetilde{R}_{D,\Delta}^{(k)},$$

so that the averaging operator is

$$E_D = \widetilde{R}_\Gamma \widetilde{R}_{D,\Gamma}^T,$$

where $\widetilde{R}_\Gamma := \widehat{R}_\Pi \oplus_{k=1}^K \widetilde{R}_\Delta^{(k)}$.

Remark 3.1. If we use a conventional averaging procedure, we start with a piecewise discrete harmonic function which is discontinuous across the interface and which is the result of solving a system with the Schur complement $\widetilde{S}$ associated with the space $\widetilde{V}_\Gamma$. By averaging pointwise across the interface, we introduce nonzero residuals next to the interface. We then remove them by solving a Dirichlet problem on each subdomain, thereby improving the performance. If we use the new deluxe averaging, we obtain one contribution from each subdomain edge/face and in other applications additional contributions, e.g., associated with the subdomain vertices. Each of them will be discrete harmonic in the subdomains, and therefore the local Dirichlet solves will no longer be necessary.

3.6. The BDDC preconditioner. We denote by $A^{(k)}$ the local stiffness matrix restricted to subdomain $\widehat{\Omega}_k$. By partitioning the local degrees of freedom into those interior (I) and those interface (Γ), as before, and by further partitioning the latter into dual (Δ) and primal (Π) degrees of freedom, $A^{(k)}$ can be written as

$$A^{(k)} = \left[\begin{array}{cc} A_{II}^{(k)} & A_{\Gamma I}^{(k)^T} \\ A_{\Gamma I}^{(k)} & A_{\Gamma\Gamma}^{(k)} \end{array} \right] = \left[\begin{array}{ccc} A_{II}^{(k)} & A_{\Delta I}^{(k)^T} & A_{\Pi I}^{(k)^T} \\ A_{\Delta I}^{(k)} & A_{\Delta\Delta}^{(k)} & A_{\Pi\Delta}^{(k)^T} \\ A_{\Pi I}^{(k)} & A_{\Pi\Delta}^{(k)} & A_{\Pi\Pi}^{(k)} \end{array} \right].$$

Using the scaled restriction matrices, defined in (3.10) and (3.14), the BDDC preconditioner can be written as

$$(3.15) \qquad M_{\text{BDDC}}^{-1} = \widetilde{R}_{D,\Gamma}^T \widetilde{S}_{\Gamma}^{-1} \widetilde{R}_{D,\Gamma},$$

where
(3.16)

$$\widetilde{S}_{\Gamma}^{-1} = \widetilde{R}_{\Gamma\Delta}^T \left(\sum_{k=1}^{K} \left[\begin{array}{cc} 0 & R_{\Delta}^{(k)^T} \end{array} \right] \left[\begin{array}{cc} A_{II}^{(k)} & A_{\Delta I}^{(k)^T} \\ A_{\Delta I}^{(k)} & A_{\Delta\Delta}^{(k)} \end{array} \right]^{-1} \left[\begin{array}{c} 0 \\ R_{\Delta}^{(k)} \end{array} \right] \right) \widetilde{R}_{\Gamma\Delta} + \Phi S_{\Pi\Pi}^{-1} \Phi^T.$$

The first term in (3.16) is the sum of local solvers on each subdomain $\widehat{\Omega}_k$, with a Neumann condition on the local Δ edges and with the coarse degrees of freedom constrained to vanish. The second term is a coarse solver for the primal variables that we have implemented as in [28, 4] by using the coarse matrix

$$S_{\Pi\Pi} = \sum_{k=1}^{K} R_{\Pi}^{(k)^T} \left(A_{\Pi\Pi}^{(k)} - \left[\begin{array}{cc} A_{\Pi I}^{(k)} & A_{\Pi\Delta}^{(k)} \end{array} \right] \left[\begin{array}{cc} A_{II}^{(k)} & A_{\Delta I}^{(k)^T} \\ A_{\Delta I}^{(k)} & A_{\Delta\Delta}^{(k)} \end{array} \right]^{-1} \left[\begin{array}{c} A_{\Pi I}^{(k)^T} \\ A_{\Pi\Delta}^{(k)^T} \end{array} \right] \right) R_{\Pi}^{(k)}$$

and a matrix Φ mapping primal degrees of freedom to interface variables, given by

$$\Phi = \widetilde{R}_{\Gamma\Pi}^T - R_{\Gamma\Delta}^T \sum_{k=1}^{K} \left[\begin{array}{cc} 0 & R_{\Delta}^{(k)^T} \end{array} \right] \left[\begin{array}{cc} A_{II}^{(k)} & A_{\Delta I}^{(k)^T} \\ A_{\Delta I}^{(k)} & A_{\Delta\Delta}^{(k)} \end{array} \right]^{-1} \left[\begin{array}{c} A_{\Pi I}^{(k)^T} \\ A_{\Pi\Delta}^{(k)^T} \end{array} \right] R_{\Pi}^{(k)}.$$

The columns of Φ represent the coarse basis functions defined as the minimum energy extension, with respect to the original bilinear form, into the subdomains and subject to the chosen set of primal constraints.

4. Condition number bounds. The condition number of the BDDC preconditioned operator can be bounded by estimating the $\widetilde{S}_{\Gamma}$-norm of the average operator defined by $E_D = \widetilde{R}_{\Gamma} \widetilde{R}_{D,\Gamma}^T$. We recall that $M_{BDDC}^{-1} = \widetilde{R}_{D,\Gamma}^T \widetilde{S}_{\Gamma}^{-1} \widetilde{R}_{D,\Gamma}$ and $\widehat{S} = \widetilde{R}_{\Gamma}^T \widetilde{S}_{\Gamma} \widetilde{R}_{\Gamma}$. The following two lemmas hold in general for any BDDC operator.

LEMMA 4.1 (lower bound).

$$(4.1) \qquad u^T M_{BDDC} u \leq u^T \widehat{S}_{\Gamma} u \quad \forall u \in \widehat{V}_{\Gamma}.$$

Proof. Let $w = M_{BDDC} u$. Since, as is easy to show, $\widetilde{R}_{\Gamma}^T \widetilde{R}_{D,\Gamma} = I$, we have

$$\begin{aligned} u^T M_{BDDC} u &\leq u^T w = u^T \widetilde{R}_{\Gamma}^T \widetilde{R}_{D,\Gamma} w = u^T \widetilde{R}_{\Gamma}^T \widetilde{S}_{\Gamma} \widetilde{S}_{\Gamma}^{-1} \widetilde{R}_{D,\Gamma} w \\ &\leq (\widetilde{R}_{\Gamma} u, \widetilde{R}_{\Gamma} u)_{\widetilde{S}_{\Gamma}}^{1/2} (\widetilde{S}_{\Gamma}^{-1} \widetilde{R}_{D,\Gamma} w, \widetilde{S}_{\Gamma}^{-1} \widetilde{R}_{D,\Gamma} w)_{\widetilde{S}_{\Gamma}}^{1/2} \\ &= (u^T \widetilde{R}_{\Gamma}^T \widetilde{S}_{\Gamma} \widetilde{R}_{\Gamma} u)^{1/2} (w^T \widetilde{R}_{D,\Gamma}^T \widetilde{S}_{\Gamma}^{-1} \widetilde{S}_{\Gamma} \widetilde{S}_{\Gamma}^{-1} \widetilde{R}_{D,\Gamma} w)^{1/2} \\ &= (u^T \widehat{S}_{\Gamma} u)^{1/2} (u^T M_{BDDC} u)^{1/2}. \quad \square \end{aligned}$$

LEMMA 4.2 (upper bound). *If $|E_D v|^2_{\widetilde{S}_\Gamma} \leq C_E |v|^2_{\widetilde{S}_\Gamma}$ for all $v \in \widetilde{V}_\Gamma$, then*

$$(4.2) \qquad u^T \widehat{S}_\Gamma u \leq C_E u^T M_{BDDC} u \quad \forall u \in \widehat{V}_\Gamma.$$

Proof.

$$
\begin{aligned}
u^T \widehat{S}_\Gamma u &= u^T \widetilde{R}_\Gamma^T \widetilde{S}_\Gamma \widetilde{R}_\Gamma u = u^T \widetilde{R}_\Gamma^T \widetilde{S}_\Gamma \widetilde{R}_\Gamma M_{BDDC}^{-1} M_{BDDC} u \\
&= u^T \widetilde{R}_\Gamma^T \widetilde{S}_\Gamma \widetilde{R}_\Gamma \widetilde{R}_{D,\Gamma}^T \widetilde{S}_\Gamma^{-1} \widetilde{R}_{D,\Gamma} w \\
&\leq (\widetilde{R}_\Gamma u, \widetilde{R}_\Gamma u)^{1/2}_{\widetilde{S}_\Gamma} (E_D \widetilde{S}_\Gamma^{-1} \widetilde{R}_{D,\Gamma} w, E_D \widetilde{S}_\Gamma^{-1} \widetilde{R}_{D,\Gamma} w)^{1/2}_{\widetilde{S}_\Gamma} \\
&\leq (u^T \widetilde{R}_\Gamma^T \widetilde{S}_\Gamma \widetilde{R}_\Gamma u)^{1/2} C_E^{1/2} (\widetilde{S}_\Gamma^{-1} \widetilde{R}_{D,\Gamma} w, \widetilde{S}_\Gamma^{-1} \widetilde{R}_{D,\Gamma} w)^{1/2}_{\widetilde{S}_\Gamma} \\
&= C_E^{1/2} (u^T \widehat{S}_\Gamma u)^{1/2} (u^T M_{BDDC} u)^{1/2},
\end{aligned}
$$

where the last step follows as in the proof of Lemma 4.1. □

4.1. The 2D case. We will make use of the following preliminary result, which is an immediate combination of Theorems 6.1 and 6.2 in [6] rewritten in the present notation.

THEOREM 4.3. *Let the dimension of the problem be equal to 2. Then for all subdomains Ω_k there exists a boundary seminorm $|\cdot|_{\overline{W}_k}$ such that for all $w^{(k)} \in V_\Gamma^{(k)}$*

$$(4.3) \qquad |w^{(k)}|^2_{\overline{W}_k} = \sum_{\mathcal{F} \in \partial \Omega} |R_\mathcal{F} w^{(k)}|^2_{\overline{W}_\mathcal{F}},$$

$$(4.4) \qquad |w^{(k)}|^2_{\overline{W}_k} \leq C \, (w^{(k)})^T S^{(k)} w^{(k)},$$

with the positive constant C independent of h, H and where $|w|_{\overline{W}_\mathcal{F}}$ is a seminorm on the space of discrete functions associated with the edge $\mathcal{F}$. Moreover, for all $w^{(k)} \in V_\Gamma^{(k)}$ that vanish at the subdomain primal (corner) degrees of freedom, it holds that

$$(4.5) \qquad (w^{(k)})^T S^{(k)} w^{(k)} \leq C(1 + \log^2(H/h))|w^{(k)}|^2_{\overline{W}_k},$$

with the positive constant C independent of h, H.

For a proof and an explicit form of this seminorm, see [6].

With these two lemmas, we can prove our main theoretical result.

THEOREM 4.4. *Consider (2.1) in two dimensions, and let the primal set be given by the subdomain corner set $\widehat{V}_\Pi^C$. Then it holds that*

$$\mathrm{cond}\Big(M_{BDDC}^{-1} \widehat{S}_\Gamma\Big) \leq C(1 + \log(H/h))^2,$$

with the positive constant C independent of h, H, and the jumps of the coefficient ρ.

Proof. Lemma 4.1 provides the lower bound $\lambda_{min}(M_{BDDC}^{-1} \widehat{S}_\Gamma) \geq 1$. Lemma 4.2 provides the upper bound $\lambda_{max}(M_{BDDC}^{-1} \widehat{S}_\Gamma) \leq C_E$ if we can prove the bound on E_D required in the hypothesis of Lemma 4.2. We will prove the equivalent bound for the complementary operator P_D defined in (3.13), and since $|E_D w|^2_{\widetilde{S}_\Gamma} = \sum_{k=1}^{K} |\bar{R}_\Gamma E_D w|^2_{S^{(k)}}$, we will focus on proving a bound for $|\bar{R}_\Gamma P_D w|^2_{S^{(k)}}$. Recalling that the deluxe average $\bar{w}_\mathcal{F}$ across an edge/face $\mathcal{F}$ shared by two subdomains has

been defined in (3.11) and that by adding the relevant contributions from the different edges/faces, the E_D and P_D operators can be written as in (3.12) and (3.13), respectively, we have

$$(4.6) \qquad |\bar{R}_\Gamma P_D w|^2_{S^{(k)}} \le |\Xi_k| \sum_{\mathcal{F} \in \Xi_k} |R_\mathcal{F}^T(w_\mathcal{F}^{(k)} - \bar{w}_\mathcal{F})|^2_{S^{(k)}},$$

where $|\Xi_k| = 4$ in our special 2D case; in the general case, we will use that the number of neighbors is finite.

Still focusing, for simplicity, on the case where $\mathcal{F}$ is shared by two subdomains (an edge in two dimensions or a face in three), we find, by simple algebra, that

$$w_\mathcal{F}^{(k)} - \bar{w}_\mathcal{F} = (S_\mathcal{F}^{(k)} + S_\mathcal{F}^{(j)})^{-1} S_\mathcal{F}^{(j)}(w_\mathcal{F}^{(k)} - w_\mathcal{F}^{(j)}),$$

so that

$$(4.7) \qquad |R_\mathcal{F}^T(w_\mathcal{F}^{(k)} - \bar{w}_\mathcal{F})|^2_{S^{(k)}} = |R_\mathcal{F}^T(S_\mathcal{F}^{(k)} + S_\mathcal{F}^{(j)})^{-1} S_\mathcal{F}^{(j)}(w_\mathcal{F}^{(k)} - w_\mathcal{F}^{(j)})|^2_{S^{(k)}}.$$

By adding and subtracting a suitable function $\hat{w} \in \widehat{V}_\Gamma$ (a specific choice will be given below), we have

$$(4.8) \quad w_\mathcal{F}^{(k)} - w_\mathcal{F}^{(j)} = w_\mathcal{F}^{(k)} - R_\mathcal{F}\hat{w} - (w_\mathcal{F}^{(j)} - R_\mathcal{F}\hat{w}) = w_\mathcal{F}^{(k)} - R_\mathcal{F}\hat{w}^{(k)} - (w_\mathcal{F}^{(j)} - R_\mathcal{F}\hat{w}^{(j)}).$$

Inserting (4.8) into (4.7) and noting that $R_\mathcal{F}S^{(k)}R_\mathcal{F}^T = S_\mathcal{F}^{(k)}$, we then find that

$$|R_\mathcal{F}^T(w_\mathcal{F}^{(k)} - \bar{w}_\mathcal{F})|^2_{S^{(k)}} = (R_\mathcal{F}^T(w_\mathcal{F}^{(k)} - \bar{w}_\mathcal{F}))^T S^{(k)}(R_\mathcal{F}^T(w_\mathcal{F}^{(k)} - \bar{w}_\mathcal{F}))$$
$$= (w_\mathcal{F}^{(k)} - w_\mathcal{F}^{(j)})^T S_\mathcal{F}^{(j)}(S_\mathcal{F}^{(k)} + S_\mathcal{F}^{(j)})^{-1} S_\mathcal{F}^{(k)}(S_\mathcal{F}^{(k)} + S_\mathcal{F}^{(j)})^{-1} S_\mathcal{F}^{(j)}(w_\mathcal{F}^{(k)} - w_\mathcal{F}^{(j)})$$
$$\le 2(w_\mathcal{F}^{(k)} - R_\mathcal{F}\hat{w}^{(k)})^T S_\mathcal{F}^{(j)}(S_\mathcal{F}^{(k)} + S_\mathcal{F}^{(j)})^{-1} S_\mathcal{F}^{(k)}(S_\mathcal{F}^{(k)} + S_\mathcal{F}^{(j)})^{-1} S_\mathcal{F}^{(j)}(w_\mathcal{F}^{(k)} - R_\mathcal{F}\hat{w}^{(k)})$$
$$+ 2(w_\mathcal{F}^{(j)} - R_\mathcal{F}\hat{w}^{(j)})^T S_\mathcal{F}^{(j)}(S_\mathcal{F}^{(k)} + S_\mathcal{F}^{(j)})^{-1} S_\mathcal{F}^{(k)}(S_\mathcal{F}^{(k)} + S_\mathcal{F}^{(j)})^{-1} S_\mathcal{F}^{(j)}(w_\mathcal{F}^{(j)} - R_\mathcal{F}\hat{w}^{(j)}).$$

We can simplify this expression by using the two inequalities

$$S_\mathcal{F}^{(j)}(S_\mathcal{F}^{(k)} + S_\mathcal{F}^{(j)})^{-1} S_\mathcal{F}^{(k)}(S_\mathcal{F}^{(k)} + S_\mathcal{F}^{(j)})^{-1} S_\mathcal{F}^{(j)} \le S_\mathcal{F}^{(k)},$$
$$S_\mathcal{F}^{(j)}(S_\mathcal{F}^{(k)} + S_\mathcal{F}^{(j)})^{-1} S_\mathcal{F}^{(k)}(S_\mathcal{F}^{(k)} + S_\mathcal{F}^{(j)})^{-1} S_\mathcal{F}^{(j)} \le S_\mathcal{F}^{(j)},$$

which follow easily by considering the action of these operators on any eigenvector of the generalized eigenvalue problem $S_\mathcal{F}^{(k)}\phi = \lambda S_\mathcal{F}^{(j)}\phi$ and just using that all eigenvalues are strictly positive. Hence, we obtain

$$(4.9) \qquad |R_\mathcal{F}^T(w_\mathcal{F}^{(k)} - \bar{w}_\mathcal{F})|^2_{S^{(k)}} \le 2(w_\mathcal{F}^{(k)} - R_\mathcal{F}\hat{w}^{(k)})^T S_\mathcal{F}^{(k)}(w_\mathcal{F}^{(k)} - R_\mathcal{F}\hat{w}^{(k)})$$
$$+ 2(w_\mathcal{F}^{(j)} - R_\mathcal{F}\hat{w}^{(j)})^T S_\mathcal{F}^{(j)}(w_\mathcal{F}^{(j)} - R_\mathcal{F}\hat{w}^{(j)}).$$

What remains, and this is where analysis rather than linear algebra enters the picture, is to establish an edge lemma which is a direct analogue to the face lemmas of [36, subsection 4.6.3] (see also [39]),

$$(4.10) \quad (w_\mathcal{F}^{(k)} - R_\mathcal{F}\hat{w}^{(k)})^T S_\mathcal{F}^{(k)}(w_\mathcal{F}^{(k)} - R_\mathcal{F}\hat{w}^{(k)}) \le C(1 + \log(H/h))^2 (w^{(k)})^T S^{(k)} w^{(k)},$$

where $w^{(k)}$ shares the values on $\mathcal{F}$ with $w_\mathcal{F}^{(k)}$ but is otherwise arbitrary. Note that this is where the logarithmic factors enter; the energy of a minimal extension will be smaller than that of the extension by zero.

To obtain the estimate (4.10), we select the function $\hat{w}$ introduced in (4.8) as the function of $\widehat{V}_\Gamma$ with the same primal values as w and with values on the edges of each Ω_k which minimizes the discrete seminorm $|\hat{w}^{(k)}|_{\overline{W}_k}$ introduced in Theorem 4.3; see also [6, equation (6.13)]. We note that, since the square of the norm $|\cdot|_{\overline{W}_k}$ is the sum of contributions from individual edges (see (4.3)), and the values at the corners, the primal degrees of freedom, are assigned, it follows immediately that this minimization problem corresponds to an edge-by-edge minimization of the seminorms $|\cdot|_{\overline{W}_\mathcal{F}}$ for all edges $\mathcal{F}$ of the subdomain partition. Therefore, $\hat{w}^{(k)}$ will be continuous across the edges; i.e., $\hat{w} \in \widehat{V}_\Gamma$. This definition guarantees that

$$(4.11) \qquad\qquad |\hat{w}^{(k)}|_{\overline{W}_k} \le |w^{(k)}|_{\overline{W}_k}.$$

Let $z_\mathcal{F}^{(k)} = w_\mathcal{F}^{(k)} - R_\mathcal{F} \hat{w}^{(k)}$. The left-hand side of (4.10) can then be bounded by

$$(4.12) \quad z_\mathcal{F}^{(k)^T} S_\mathcal{F}^{(k)} z_\mathcal{F}^{(k)} = (R_\mathcal{F}^T z_\mathcal{F}^{(k)})^T S^{(k)} (R_\mathcal{F}^T z_\mathcal{F}^{(k)}) \le C_1 (1 + \log(H/h))^2 |R_\mathcal{F}^T z_\mathcal{F}^{(k)}|_{\overline{W}_k}^2,$$

where we have used (4.5). Since $R_\mathcal{F}^T z_\mathcal{F}^{(k)} = R_\mathcal{F}^T (w_\mathcal{F}^{(k)} - R_\mathcal{F} \hat{w}^{(k)}) = R_\mathcal{F}^T R_\mathcal{F} (w^{(k)} - \hat{w}^{(k)})$ is nonzero only on the edge $\mathcal{F}$ and the discrete seminorm $|\cdot|_{\overline{W}_k}$ is defined edge-by-edge as a sum of four terms, only that associated with the common edge $\mathcal{F}$ is nonzero. Hence, by using (4.11), we have

$$|R_\mathcal{F}^T z_\mathcal{F}^{(k)}|_{\overline{W}_k}^2 \le |w^{(k)} - \hat{w}^{(k)}|_{\overline{W}_k}^2 \le 2(|w^{(k)}|_{\overline{W}_k}^2 + |\hat{w}^{(k)}|_{\overline{W}_k}^2) \le 4|w^{(k)}|_{\overline{W}_k}^2.$$

By (4.4), we can then return to the local Schur bilinear form

$$|w^{(k)}|_{\overline{W}_k}^2 \le C w^{(k)^T} S^{(k)} w^{(k)},$$

and obtain the edge lemma (4.10).

We can also compute, in exactly the same way, the contribution of the other subdomain Ω_j as well as contributions from other relevant subdomain edges or faces. Summing over the edges of Ω_k, we obtain from (4.6), (4.9), and (4.10)

$$|\bar{R}_\Gamma P_D w|_{S^{(k)}}^2 \le C(1 + \log(H/h))^2 \sum_{j \in \Xi_k \cup \{k\}} |w^{(j)}|_{S^{(j)}}^2$$

and hence the same bound on $|\bar{R}_\Gamma E_D w|_{S^{(k)}}^2$, and summing over the subdomains, we have

$$(4.13) \qquad\qquad |E_D w|_{\widetilde{S}_\Gamma}^2 \le C(1 + \log(H/h))^2 |w|_{\widetilde{S}_\Gamma}^2,$$

i.e., the E_D bound required by Lemma 4.2 with $C_E = C(1 + \log(H/h))^2$, which proves the theorem. $\square$

Remark 4.1. In IGA the domain of interest is often not described by a single mapped patch but is built by gluing together (with C^0 or C^1 regularity) multiple NURBS patches. The case of multipatch domains fits very naturally into the present description. Indeed, if each single patch is treated as a single subdomain, this is equivalent to the case with C^0 (or C^1) regularity across the interface Γ. If the patches are subdivided into more than one subdomain, then some interface edges will be C^0/C^1 and others may have any C^κ regularity. The same observation applies to the regularity across the edges of the Bezier elements inside the subdomains, which can clearly be independent from the regularity across the subdomain (and patch) interfaces.

4.2. The case of more than two subspaces. We have shown above how to reduce an estimate of the norm of $w_{\mathcal{F}}^{(k)} - \bar{w}_{\mathcal{F}}$ for the case of an equivalence class associated with just two subdomains. In many cases, we also need to work with equivalence classes with three or more subdomains; this is, e.g., the case if some of the degrees of freedom associated with the set Ω_C are not primal, as for the reduced primal set $\widehat{V}_{\Pi}^{C_4}$ described below. This is also necessary for 3D problems unless we make the many degrees of freedom associated with all fat subdomain edges primal.

We will first show that the same algebraic ideas can be used to take care of the case of three subdomains, $\Omega_{k_1}, \Omega_{k_2}$, and Ω_{k_3}, and an edge $\mathcal{E}$.

Letting $S_{\mathcal{E}}^{(k_{123})} := S_{\mathcal{E}}^{(k_1)} + S_{\mathcal{E}}^{(k_2)} + S_{\mathcal{E}}^{(k_3)}$, our averaging operator now has the form

$$\bar{w}_{\mathcal{E}} := (S_{\mathcal{E}}^{(k_{123})})^{-1}(S_{\mathcal{E}}^{(k_1)}w_{\mathcal{E}}^{(k_1)} + S_{\mathcal{E}}^{(k_2)}w_{\mathcal{E}}^{(k_2)} + S_{\mathcal{E}}^{(k_3)}w_{\mathcal{E}}^{(k_3)}).$$

As before, the required Schur complements can be computed explicitly if they have small dimensions; otherwise their action can be computed by solving Dirichlet problems on the union of the relevant subdomains. We find that

$$w_{\mathcal{E}} - \bar{w}_{\mathcal{E}} = (S_{\mathcal{E}}^{(k_{123})})^{-1}((S_{\mathcal{E}}^{(k_2)} + S_{\mathcal{E}}^{(k_3)})w_{\mathcal{E}}^{(k_1)} - S_{\mathcal{E}}^{(k_2)}w_{\mathcal{E}}^{(k_2)} - S_{\mathcal{E}}^{(k_3)}w_{\mathcal{E}}^{(k_3)}).$$

Since $R_{\mathcal{E}}S^{(k_1)}R_{\mathcal{E}}^T = S_{\mathcal{E}}^{(k_1)}$, then the analogue of (4.7) for three subdomains becomes

$$|R_{\mathcal{E}}^T(w_{\mathcal{E}}^{(k_1)}-\bar{w}_{\mathcal{E}})|_{S^{(k_1)}}^2 = |(S_{\mathcal{E}}^{(k_{123})})^{-1}((S_{\mathcal{E}}^{(k_2)}+S_{\mathcal{E}}^{(k_3)})w_{\mathcal{E}}^{(k_1)}-S_{\mathcal{E}}^{(k_2)}w_{\mathcal{E}}^{(k_2)}-S_{\mathcal{E}}^{(k_3)}w_{\mathcal{E}}^{(k_3)})|_{S_{\mathcal{E}}^{(k_1)}}^2.$$

This norm can be bounded from above by the sum of the three terms:

(4.14)
$$\begin{aligned}
&3w_{\mathcal{E}}^{(k_1)T}(S_{\mathcal{E}}^{(k_2)} + S_{\mathcal{E}}^{(k_3)})(S_{\mathcal{E}}^{(k_{123})})^{-1}S_{\mathcal{E}}^{(k_1)}(S_{\mathcal{E}}^{(k_{123})})^{-1}(S_{\mathcal{E}}^{(k_2)} + S_{\mathcal{E}}^{(k_3)})w_{\mathcal{E}}^{(k_1)} \\
&+ 3w_{\mathcal{E}}^{(k_2)T}S_{\mathcal{E}}^{(k_2)}(S_{\mathcal{E}}^{(k_{123})})^{-1}S_{\mathcal{E}}^{(k_1)}(S_{\mathcal{E}}^{(k_{123})})^{-1}S_{\mathcal{E}}^{(k_2)}w_{\mathcal{E}}^{(k_2)} \\
&+ 3w_{\mathcal{E}}^{(k_3)T}S_{\mathcal{E}}^{(k_3)}(S_{\mathcal{E}}^{(k_{123})})^{-1}S_{\mathcal{E}}^{(k_1)}(S_{\mathcal{E}}^{(k_{123})})^{-1}S_{\mathcal{E}}^{(k_3)}w_{\mathcal{E}}^{(k_3)}.
\end{aligned}$$

The first term can be bounded by $3w_{\mathcal{E}}^{(k_1)T}S_{\mathcal{E}}^{(k_1)}w_{\mathcal{E}}^{(k_1)}$ by using the same argument as in the case of two subdomains and by working with $S_{\mathcal{E}}^{(k_1)}$ and $S_{\mathcal{E}}^{(k_2)} + S_{\mathcal{E}}^{(k_3)}$.

The second expression can also be reduced to an argument with the two matrices, $S_{\mathcal{E}}^{(k_2)}$ and $S_{\mathcal{E}}^{(k_1)} + S_{\mathcal{E}}^{(k_3)}$, after first bounding it from above by

$$3w_{\mathcal{E}}^{(k_2)T}S_{\mathcal{E}}^{(k_2)}(S_{\mathcal{E}}^{(k_{123})})^{-1}(S_{\mathcal{E}}^{(k_1)} + S_{\mathcal{E}}^{(k_3)})(S_{\mathcal{E}}^{(k_{123})})^{-1}S_{\mathcal{E}}^{(k_2)}w_{\mathcal{E}}^{(k_2)}.$$

A bound of $3w_{\mathcal{E}}^{(k_2)T}S_{\mathcal{E}}^{(k_2)}w_{\mathcal{E}}^{(k_2)}$ results.

The third expression can be bounded by $3w_{\mathcal{E}}^{(k_3)T}S_{\mathcal{E}}^{(k_3)}w_{\mathcal{E}}^{(k_3)}$ in the same way. Subtracting a common element of the primal space from $w_{\mathcal{E}}^{(k_1)}, w_{\mathcal{E}}^{(k_2)}$, and $w_{\mathcal{E}}^{(k_3)}$, as in the case of two subdomains, we then obtain the analogue of (4.9):

(4.15)
$$\begin{aligned}
|R_{\mathcal{E}}^T(w_{\mathcal{E}}^{(k_1)} - \bar{w}_{\mathcal{E}})|_{S^{(k_1)}}^2 \leq\; &3(w_{\mathcal{E}}^{(k_1)} - R_{\mathcal{E}}\hat{w}^{(k_1)})^T S_{\mathcal{E}}^{(k_1)}(w_{\mathcal{E}}^{(k_1)} - R_{\mathcal{E}}\hat{w}^{(k_1)}) \\
&+ 3(w_{\mathcal{E}}^{(k_2)} - R_{\mathcal{E}}\hat{w}^{(k_2)})^T S_{\mathcal{E}}^{(k_2)}(w_{\mathcal{E}}^{(k_2)} - R_{\mathcal{E}}\hat{w}^{(k_2)}) \\
&+ 3(w_{\mathcal{E}}^{(k_3)} - R_{\mathcal{E}}\hat{w}^{(k_3)})^T S_{\mathcal{E}}^{(k_3)}(w_{\mathcal{E}}^{(k_3)} - R_{\mathcal{E}}\hat{w}^{(k_3)}).
\end{aligned}$$

Each of these terms can then be bounded by a counterpart of the edge lemma (4.10).

Turning to the four subdomain case, we have

$$\bar{w}_{\mathcal{E}}^{(k_1)} := (S_{\mathcal{E}}^{(k_{1234})})^{-1}(S_{\mathcal{E}}^{(k_1)}w_{\mathcal{E}}^{(k_1)} + S_{\mathcal{E}}^{(k_2)}w_{\mathcal{E}}^{(k_2)} + S_{\mathcal{E}}^{(k_3)}w_{\mathcal{E}}^{(k_3)} + S_{\mathcal{E}}^{(k_4)}w_{\mathcal{E}}^{(k_4)}),$$

where $S_{\mathcal{E}}^{(k_{1234})} := S_{\mathcal{E}}^{(k_1)} + S_{\mathcal{E}}^{(k_2)} + S_{\mathcal{E}}^{(k_3)} + S_{\mathcal{E}}^{(k_4)}$, and we find that $w_{\mathcal{E}}^{(k_1)} - \bar{w}_{\mathcal{E}}^{(k_1)}$ equals

$$(S_{\mathcal{E}}^{(k_{1234})})^{-1}((S_{\mathcal{E}}^{(k_2)} + S_{\mathcal{E}}^{(k_3)} + S_{\mathcal{E}}^{(k_4)})w_{\mathcal{E}}^{(k_1)} - S_{\mathcal{E}}^{(k_2)}w_{\mathcal{E}}^{(k_2)} - S_{\mathcal{E}}^{(k_3)}w_{\mathcal{E}}^{(k_3)} - S_{\mathcal{E}}^{(k_4)}w_{\mathcal{E}}^{(k_4)}).$$

The norm $|R_{\mathcal{E}}^T(w_{\mathcal{E}}^{(k_1)} - \bar{w}_{\mathcal{E}})|^2_{S^{(k_1)}}$ can then be bounded, by using the same arguments as for three subdomains, by the sum of four terms, each with a coefficient 4.

4.3. A reduced primal set. In case of maximal regularity $\kappa = p - 1$ of the isogeometric basis functions, the fat interface leads to a rich primal set $\widehat{V}_{\Pi}^C$ with p^2 primal degrees of freedom for each subdomain vertex in two dimensions. We can then consider a reduced primal set $\widehat{V}_{\Pi}^{C_4}$ where out of these p^2 degrees of freedom per vertex only the four corner degrees of freedom are retained as primal and the other $p^2 - 4$ are considered dual. For this reduced primal set, we expect the same scalable convergence bound of Theorem 4.4, since the presence of two primal corners per edge still allow us to prove an edge lemma (see the proof of Theorem 4.3 that can be found in [6]), and the additional $p^2 - 4$ dual variables per vertex are now shared by four subdomains and can be treated with the techniques of section 4.2. The numerical results presented in section 5 confirm this scalable bound but also show that the BDDC convergence rate with the primal set $\widehat{V}_{\Pi}^{C_4}$ deteriorates rapidly with an increasing p.

4.4. The 3D case. We conjecture that a scalable convergence bound as in Theorem 4.4 holds also in three dimensions, but a complete proof is beyond the scope of this paper. We only note that the basic tools required are isogeometric edge and face lemmas in three dimensions, which we believe can be obtained by extending the 2D isogeometric techniques of our previous work [6] and the deluxe estimates in the case of more than two subdomains considered in section 4.2.

5. Numerical results. In this section, we report on numerical experiments with the isogeometric BDDC deluxe preconditioner for 2D and 3D elliptic model problems (2.1) on both the parametric (reference square or cube) and physical domains, discretized with isogeometric NURBS spaces with a mesh size h, polynomial degree p, and regularity κ. The domain is decomposed into K nonoverlapping subdomains of characteristic size H, as described in section 3. In the following, we will denote by $\kappa_\Gamma \leq \kappa$ the regularity at the subdomain interfaces. The discrete Schur complement problems are solved by the PCG method with the isogeometric BDDC preconditioner, with a zero initial guess and a stopping criterion of a 10^{-6} reduction of the Euclidean norm of the PCG residual. In the tests, we study how the convergence rate of the BDDC preconditioner depends on $h, K, p, \kappa, \kappa_\Gamma$ and jumps in the coefficient of the elliptic problem. In all tests, the BDDC condition number is essentially the maximum eigenvalue of the preconditioned operator, since its minimum eigenvalue is always very close to 1. The 2D tests have been performed with a MATLAB code based on the GeoPDEs library [13], while the 3D tests have been performed using the PETSc library [1] and its PCBDDC preconditioner (contributed to the PETSc library by S. Zampini), and run on the BlueGene/Q cluster of the CINECA Laboratory (http://www.hpc.cineca.it/hardware/ibm-bgq-fermi).

An efficient implementation of the deluxe operator in a parallel environment requires the construction of a face-centered adjacency graph of the interface equivalence classes. In this graph, a vertex corresponds to an edge or a face of the interface and two vertices are connected if and only if they belong to the same subdomain. Each local problem required by the application of the deluxe operator is associated with a vertex of the graph. We color this graph with a distance-one coloring, where two

TABLE 1
Number of deluxe subproblems and colors needed as a function of the number of subdomains $K = n \times n \times n$.

K	2^3	3^3	4^3	5^3	6^3	7^3	8^3
problems	18	90	252	540	990	1638	2520
colors	6	18	18	19	18	20	19
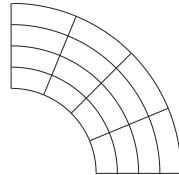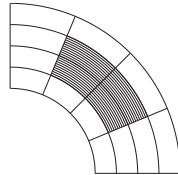
(a) homogeneous   (b) central jump   (c) checkerboard
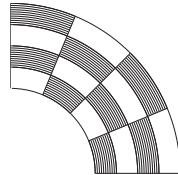
FIG. 2. *2D quarter-ring domains used in the numerical tests. Examples with 4×4 subdomains.*

adjacent vertices do not have the same color. Then the application of the deluxe operator can be efficiently solved in parallel on subcommunicators associated with different colors. The number of steps required to solve all deluxe subproblems equals the number of colors, whereas the number of deluxe subproblems increases as the number of subdomains increases. Table 1 reports on the number of colors and deluxe subproblems for 3D parallelepipedal domains Ω decomposed into $K = n \times n \times n$ subdomains, which is the minimum number of colors needed to color a graph when $n > 2$ is 18, with 6 faces and 12 edges of the subdomains, which do not touch $\partial\Omega$. In order to color the adjacency graph of deluxe subproblems in our code we have used the Colpack library (http://cscapes.cs.purdue.edu/coloringpage/index.htm), written in C++ and based on the Standard Template Library.

We first report on results of 2D experiments with deluxe BDDC with the primal set $\widehat{V}_\Pi^C$ for all the subdomain vertices. In the 3D experiments, we will consider the primal sets defined in section 3.4, consisting of subdomain vertices ($\widehat{V}_\Pi^C$), or subdomain vertices and edge averages ($\widehat{V}_\Pi^{C+E}$), or subdomain vertices and edge and face averages ($\widehat{V}_\Pi^{C+E+F}$). We consider the richer sets where each fat edge/face is decomposed into slim edges/faces parallel to the subdomain edge/face and one average is computed over each such edge/face.

5.1. Scalability in K and quasi-optimality in H/h in two dimensions. The condition number cond, defined as the ratio of the maximum and minimum eigenvalues of $M_{BDDC}^{-1}\widehat{S}_\Gamma$, and iteration counts n_{it} of the BDDC deluxe preconditioner are reported in Table 2 for a quarter-ring domain (see Figure 2(a)) as a function of the number of subdomains K and mesh size h for fixed $p = 3, \kappa = 2$ (top) or $p = 5, \kappa = 4$ (bottom). The results show that the proposed preconditioner is scalable, since, moving along the diagonals of each table, the condition number appears to be bounded from above by a constant independent of K. The results for higher degree $p = 5$ and regularity $\kappa = 4$ are even better than those for the lower degree case. In contrast to the scalings proposed in our previous work [6], the BDDC deluxe preconditioner appears to retain a very good performance in spite of the increase of the polynomial degree p. To better understand this issue, we next study the BDDC performance for increasing values of p.

TABLE 2

BDDC deluxe preconditioner for a 2D quarter-ring domain: Condition number cond *and iteration counts* n_{it} *as a function of the number of subdomains K and mesh size h. Fixed* $p = 3, \kappa = 2$ *(top),* $p = 5, \kappa = 4$ *(bottom).*

		$h = 1/16$		$h = 1/32$		$h = 1/64$		$h = 1/128$	
	K	cond	n_{it}	cond	n_{it}	cond	n_{it}	cond	n_{it}
	2×2	1.24	5	1.42	6	1.65	6	1.92	6
$p = 3$	4×4			2.02	8	2.68	10	3.46	11
$\kappa = 2$	8×8					2.39	10	3.29	12
	16×16							2.64	11
	2×2	1.19	5	1.35	6	1.55	6	1.78	6
$p = 5$	4×4			1.62	8	2.19	9	2.86	10
$\kappa = 4$	8×8					1.77	8	2.55	10
	16×16							1.87	8

TABLE 3

BDDC deluxe dependence on p in the 2D quarter-ring domain: Condition number cond *and iteration counts* n_{it} *as a function of the spline degree p. Fixed* $h = 1/64, K = 4 \times 4, \kappa = p - 1.$

p	2	3	4	5	6	7	8	9	10
cond	3.22	2.68	2.41	2.19	2.04	1.91	1.80	1.72	1.62
n_{it}	10	10	9	9	9	8	8	8	9

5.2. Dependence on p in two dimensions. In this test, we compare the BDDC deluxe performance as a function of the polynomial degree p and the regularity κ. We recall that our theoretical work in section 4 is only an h-analysis and does not cover the dependence of the convergence rate on p and κ. The domain considered is the quarter-ring of Figure 2(a) discretized with a mesh size $h = 1/64$ and $K = 4 \times 4$ subdomains, while the degree p varies from 2 to 10 and the regularity $\kappa = p - 1$ is maximal everywhere. The results in Table 3 show that the condition numbers and iteration counts are bounded independently of the degree p and actually improve slightly for increasing p. These remarkable results are a considerable improvement over the results in p with ρ and stiffness scaling of our previous work (see Tables 4 and 5 of [6]), especially taking into account that the latter were obtained only for low regularity at the subdomain interface, $\kappa_\Gamma = 0, 1$, while here the regularity $\kappa = p - 1$ is maximal everywhere.

5.3. Robustness with respect to discontinuous coefficients in two dimensions. We next investigate the robustness of the BDDC deluxe preconditioner with respect to jump discontinuities of the coefficient ρ of the elliptic problem (2.1). We consider three different tests, which we call "central jump," "random mix," and "checkerboard," on a 2D quarter-ring domain decomposed into 4×4 subdomains; see Figure 2. In the central jump test, ρ varies by eight orders of magnitude (from 10^{-4} to 10^4) in the 2×2 central subdomains, while it equals 1 in the surrounding subdomains. In the random mix test, ρ has random values varying by eight orders of magnitude in the different subdomains; see Figure 3 (upper part) for the values of ρ in the parametric space. In the checkerboard test, $\rho = 10^4$ in the black subdomains, while $\rho = 1$ in the white subdomains. We fix $h = 1/64$, $H/h = 16$, $p = 3$, $\kappa = 2$, and the regularity at the subdomain interfaces $\kappa_\Gamma = 0$, since in the presence of jumps in the elliptic coefficient this is the correct choice for approximation reasons; see, e.g., [8]. The condition numbers and iteration counts reported in the tables of Figure 3 clearly show the robustness of BDDC deluxe, since cond and n_{it} are essentially independent of the jumps in ρ.

Central jump

1	1	1	1
1	ρ	ρ	1
1	ρ	ρ	1
1	1	1	1

Random mix

10^{-3}	10^2	10^{-4}	10^2
10^1	10^{-1}	10^0	10^4
10^{-2}	10^3	10^2	10^{-4}
10^0	10^4	10^{-3}	10^1

Central jump

ρ	cond	n_{it}
10^{-4}	5.41	13
10^{-2}	5.42	13
1	5.94	13
10^2	7.18	13
10^4	7.26	13

Random mix

cond	n_{it}
5.25	11

Checkerboard

cond	n_{it}
5.11	14

FIG. 3. *BDDC deluxe robustness with respect to jump discontinuities in the coefficient ρ of the elliptic problem. Central jump, random mix and checkerboard tests. Condition number* cond *and CG iteration counts* n_{it} *Fixed $h = 1/64$, $K = 4 \times 4$, $H/h = 16$.*

TABLE 4

Optimality, scalability, and dependence on p of the BDDC deluxe preconditioner with reduced primal set $\widehat{V}_\Pi^{C_4}$ in the 2D quarter of ring domain: Condition number cond *and CG iteration counts* n_{it}. *The spline regularity κ is always maximal; i.e., $\kappa = p - 1$.*

Quasi-optimality $p = 3$, $K = 2 \times 2$			Scalability $p = 3$, $H/h = 8$			Dependence on p $h = 1/64$, $K = 4 \times 4$		
H/h	cond	n_{it}	K	cond	n_{it}	p	cond	n_{it}
8	3.67	8	2×2	3.67	8	2	16.03	15
16	3.67	8	4×4	43.49	16	3	56.70	14
32	3.66	9	8×8	46.02	27	4	967.40	20
64	4.19	9	16×16	46.58	29	5	11415.81	22

5.4. Performance for the reduced primal set $\widehat{V}_\Pi^{C_4}$ in two dimensions. We study the optimality, scalability, and dependence on a growing p of the BDDC deluxe preconditioner, with the reduced primal set $\widehat{V}_\Pi^{C_4}$ defined in section 4.3, on the 2D quarter of a ring domain. The spline regularity κ is kept maximal, i.e., $\kappa = p - 1$. The results reported in Table 4 show that, in accordance with the theoretical estimate, the BDDC deluxe preconditioner is optimal and scalable also with the reduced primal set $\widehat{V}_\Pi^{C_4}$ but that the behavior with respect to increasing p is much worse than with the rich primal set $\widehat{V}_\Pi^C$.

5.5. Scalability in K in three dimensions. We next report on 3D parallel tests on a BlueGene/Q machine, assigning one subdomain per processor. We start with weak scalability tests on the unit cube: we increase the number of subdomains $K = 2^3, \ldots, 10^3$, keeping the local size $H/h = 8$ fixed, polynomial degree $p = 3$, and maximum regularity $\kappa = 2$. We consider three primal spaces of increasing size consisting of subdomain vertices ($\widehat{V}_\Pi^C$), subdomain vertices and edge averages ($\widehat{V}_\Pi^{C+E}$), or subdomain vertices and edge and face averages ($\widehat{V}_\Pi^{C+E+F}$). The results reported in Table 5 show that BDDC with both deluxe scaling (top) and stiffness scaling (bottom) of [6] are scalable, since the condition numbers and iteration counts are bounded from above by constants independent of the number of subdomains. As expected, larger primal spaces yield faster convergence rates. Deluxe scaling performs better than stiffness scaling in all tests, requiring about half the iteration counts. We remark

TABLE 5

BDDC weak scalability on the unit cube with different coarse spaces. Deluxe scaling (top), stiffness scaling (bottom). Condition number cond *and iteration counts* n_{it} *as a function of the number of subdomains* $K = n \times n \times n$*; fixed* $\kappa = 2, p = 3, H/h = 8$.

	K	2^3	3^3	4^3	5^3	6^3	7^3	8^3	9^3	10^3
		Deluxe scaling								
$\widehat{V}_\Pi^C$	cond	8.96	8.38	8.44	8.38	8.35	8.35	8.35	8.36	8.35
	n_{it}	20	21	23	24	23	23	24	24	24
$\widehat{V}_\Pi^{C+E}$	cond	2.06	2.01	1.98	1.98	1.98	1.98	1.98	1.98	1.98
	n_{it}	10	11	11	10	10	10	10	10	10
$\widehat{V}_\Pi^{C+E+F}$	cond	1.42	1.40	1.41	1.40	1.40	1.40	1.40	1.40	1.40
	n_{it}	8	8	8	8	8	8	8	8	8
		Stiffness scaling								
$\widehat{V}_\Pi^C$	cond	20.09	19.24	19.16	19.16	19.16	19.16	19.16	19.16	19.17
	n_{it}	26	33	38	39	39	39	39	39	39
$\widehat{V}_\Pi^{C+E}$	cond	6.04	6.08	6.08	6.10	6.09	6.10	6.09	6.10	6.10
	n_{it}	21	22	22	22	22	23	22	23	22
$\widehat{V}_\Pi^{C+E+F}$	cond	6.04	6.08	6.08	6.10	6.09	6.10	6.09	6.10	6.10
	n_{it}	21	22	22	22	22	23	22	23	22

TABLE 6

BDDC dependence on H/h*, unit cube. Condition number* cond *and PCG iteration counts* n_{it}*. Fixed* $p = 3, \kappa = 2, K = 4 \times 4 \times 4$*. The void columns could not be run due to memory limitations.*

	H/h	4	8	12	16	20	24
		Deluxe scaling					
$\widehat{V}_\Pi^C$	cond	2.62	6.13	10.10	14.19	17.91	—
	n_{it}	12	18	21	24	27	—
$\widehat{V}_\Pi^{C+E}$	cond	1.54	1.80	2.03	2.21	2.35	—
	n_{it}	9	10	11	12	12	—
$\widehat{V}_\Pi^{C+E+F}$	cond	1.54	1.37	1.46	1.62	1.75	—
	n_{it}	9	8	8	9	9	—
		Stiffness scaling					
$\widehat{V}_\Pi^C$	cond	7.03	10.59	21.30	34.64	46.97	66.86
	n_{it}	24	26	34	40	46	54
$\widehat{V}_\Pi^{C+E}$	cond	6.35	6.09	6.13	6.26	8.15	10.28
	n_{it}	23	22	22	23	26	29
$\widehat{V}_\Pi^{C+E+F}$	cond	6.35	6.09	6.13	6.16	6.19	6.21
	n_{it}	23	22	22	21	22	22

that BDDC deluxe yields quite small condition numbers, being bounded by 9 for the primal space $\widehat{V}_\Pi^C$, by 2 for $\widehat{V}_\Pi^{C+E}$, and by 1.4 for $\widehat{V}_\Pi^{C+E+F}$.

5.6. Quasi-optimality in H/h in three dimensions. Table 6 reports the results of parallel tests with increasing values of $H/h = 4, 8, \ldots, 24$ for fixed $p = 3$, $\kappa = 2$, and $4 \times 4 \times 4$ subdomains. Since the domain and its subdivision are fixed ($H = 1/4$), here we are varying the mesh size h. We consider again the primal spaces $\widehat{V}_\Pi^C$, $\widehat{V}_\Pi^{C+E}$, and $\widehat{V}_\Pi^{C+E+F}$ and deluxe scaling (top) and stiffness scaling (bottom). The results show a linear dependence of the condition number on H/h for the primal space $\widehat{V}_\Pi^C$, both for stiffness and deluxe scaling. The addition of edge averages ($\widehat{V}_\Pi^{C+E}$) seems sufficient to obtain a quasi-optimal method. Again deluxe scaling requires half (or less than half) the iterations of stiffness scaling.

TABLE 7

BDDC dependence on p for the 3D unit cube with different coarse spaces and deluxe scaling. Condition number cond *and iteration counts* n_{it} *as a function of the polynomial degree p. Fixed* $h = 1/24, K = 2 \times 2 \times 2, \kappa = p - 1$.

	p	2	3	4	5	6	7
		Deluxe scaling					
$\widehat{V}_\Pi^C$	cond	5.62	4.71	4.39	3.92	5.12	11.15
	n_{it}	12	11	12	14	18	26
$\widehat{V}_\Pi^{C+E}$	cond	2.10	1.91	2.03	2.68	4.99	10.92
	n_{it}	10	9	10	12	17	26
$\widehat{V}_\Pi^{C+E+F}$	cond	1.58	1.45	1.70	2.68	4.99	10.92
	n_{it}	8	8	9	12	17	26

TABLE 8

BDDC deluxe robustness with respect to jump discontinuities in the diffusion coefficient ρ. Unit cube with central jump, random mix, and checkerboard tests. Condition number cond *and PCG iteration counts* n_{it}. *Fixed* $h = 1/32, p = 3, C^0$ *continuity at the interface,* $4 \times 4 \times 4$ *subdomains.*

	ρ	Central jump cond	n_{it}	Checkerboard cond	n_{it}	Random mix cond	n_{it}
	10^{-4}	117.37	44	—	—	—	—
	10^{-2}	118.40	44	—	—	—	—
$\widehat{V}_\Pi^C$	1	134.04	48	134.04	48	134.04	48
	10^2	137.15	50	102.11	43	126.53	47
	10^4	137.40	52	104.31	44	123.63	46
	10^{-4}	5.33	18	—	—	—	—
	10^{-2}	5.33	18	—	—	—	—
$\widehat{V}_\Pi^{C+E}$	1	5.27	18	5.27	18	5.27	18
	10^2	4.92	16	4.19	16	4.83	16
	10^4	4.88	16	4.20	16	4.87	16
	10^{-4}	1.98	10	1.98	10	—	—
	10^{-2}	1.99	10	1.99	10	—	—
$\widehat{V}_\Pi^{C+E+F}$	1	2.05	10	2.05	10	2.05	10
	10^2	2.05	10	2.05	10	2.00	10
	10^4	2.05	10	2.05	10	2.00	9

5.7. Dependence on p in three dimensions. In this test, we study the BDDC convergence rate for increasing polynomial degree $p = 2, 3, \ldots, 7$ and maximal regularity $\kappa = p - 1$. The domain considered is the unit cube, with mesh size $h = 1/24$, subdivided into $K = 2 \times 2 \times 2$ subdomains. The results reported in Table 7 show that the condition numbers and iteration counts using deluxe scaling (top table) are almost independent of p for $p \leq 5$; when $p > 5$, the convergence rate of deluxe BDDC begins to degrade but is still orders of magnitude better than that of BDDC with stiffness scaling (not shown). Interestingly, the condition number of the vertex-only coarse space becomes closer to those of the other coarse spaces when using deluxe scaling with higher polynomial degrees. The addition of the face averages to the primal space marginally improves the condition number only when $p \leq 4$.

5.8. Robustness with respect to discontinuous coefficients in three dimensions. The results of parallel tests with discontinuous coefficient ρ are reported in Table 8 for a unit cube discretized with $H/h = 8$, $p = 3$, $\kappa_\Gamma = 0$ continuity at the interface, and $4 \times 4 \times 4$ subdomains. The distribution of values of ρ is the 3D analogue of the 2D case, i.e., "central jump," "checkerboard," and "random mix." The random setting is somewhat different from the 2D case; given a value of ρ, a random

TABLE 9

BDDC weak scalability on the twisted bar domains (left) with different coarse spaces. Deluxe scaling (top), stiffness scaling (bottom). Condition number cond *and iteration counts* n_{it} *as a function of the number of subdomains* $K = n \times n \times n$; *fixed* $\kappa = 2, p = 3, H/h = 6$.
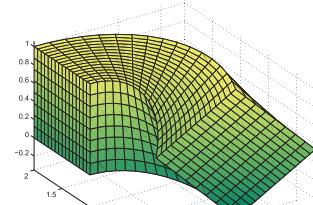
	K	2^3	3^3	4^3	5^3	6^3
		Deluxe scaling				
$\widehat{V}_\Pi^C$	cond	3.94	5.72	6.87	7.47	7.83
	n_{it}	11	15	20	21	23
$\widehat{V}_\Pi^{C+E}$	cond	1.67	1.81	1.85	1.86	1.92
	n_{it}	9	10	10	10	10
$\widehat{V}_\Pi^{C+E+F}$	cond	1.42	1.58	1.66	1.72	1.76
	n_{it}	8	9	9	9	9
		Stiffness scaling				
$\widehat{V}_\Pi^C$	cond	9.39	11.07	12.97	13.87	14.39
	n_{it}	24	29	30	31	33
$\widehat{V}_\Pi^{C+E}$	cond	8.94	9.21	9.27	9.35	9.38
	n_{it}	24	27	28	28	29
$\widehat{V}_\Pi^{C+E+F}$	cond	8.94	9.21	9.27	9.35	9.38
	n_{it}	24	27	28	28	29

number r in the interval $(-\log_{10}\rho, \log_{10}\rho)$ is generated for each subdomain, and the scaling factor for that subdomain is chosen as 10^r. In the checkerboard case, the local matrices are scaled by ρ on black subdomains and by $1/\rho$ on white subdomains. Note that the rows associated with a value of $\rho < 1$ for the checkerboard and random test cases are void since these cases are already covered by the rows corresponding to the reciprocal of the ρ value. The results clearly show the BDDC robustness with respect to jumps in ρ. The convergence rate with the primal space $\widehat{V}_\Pi^C$ is somewhat unsatisfactory, but $\widehat{V}_\Pi^{C+E}$ and especially $\widehat{V}_\Pi^{C+E+F}$ yield remarkably small condition numbers and low iteration counts.

5.9. 3D scalability on deformed domains. Finally, Table 9 illustrates the BDDC weak scalability on the deformed domains shown on the left of the table, a twisted and bent bar. The table reports cond and n_{it} for deluxe scaling (top) and stiffness scaling (bottom) for the same three coarse spaces considered before. In this weak scaling test, the number of subdomains K increases from 2^3 to 6^3 for fixed $\kappa = 2, p = 3, H/h = 6$. The results are analogous to the weak scaling test for the cube of Table 5; all three coarse spaces appear to be scalable, with deluxe scaling performing better than stiffness scaling, and with remarkably small condition numbers for deluxe scaling with the richer coarse spaces $\widehat{V}_\Pi^{C+E}$ and $\widehat{V}_\Pi^{C+E+F}$.

REFERENCES

[1] S. BALAY, J. BROWN, K. BUSCHELMAN, W. D. GROPP, D. KAUSHIK, M. G. KNEPLEY, L. CURF-MAN MCINNES, B. F. SMITH, AND H. ZHANG, *PETSc Web page*, http://www.mcs.anl.gov/petsc (2012).
[2] Y. BAZILEVS, L. BEIRÃO DA VEIGA, J. A. COTTRELL, T. J. R. HUGHES, AND G. SANGALLI, *Isogeometric analysis: Approximation, stability and error estimates for h-refined meshes*, Math. Models Methods Appl. Sci., 16 (2006), pp. 1–60.
[3] L. BEIRÃO DA VEIGA, A. BUFFA, G. SANGALLI, AND R. VAZQUEZ, *Mathematical analysis of variational isogeometric methods*, Acta Numer., to appear.
[4] L. BEIRÃO DA VEIGA, C. CHINOSI, C. LOVADINA, AND L. F. PAVARINO, *Robust BDDC preconditioners for Reissner–Mindlin plate bending problems and MITC elements*, SIAM J. Numer. Anal., 47 (2010), pp. 4214–4238.

[5] L. Beirão da Veiga, D. Cho, L. F. Pavarino, and S. Scacchi, *Overlapping Schwarz methods for Isogeometric Analysis*, SIAM J. Numer. Anal., 50 (2012), pp. 1394–1416.

[6] L. Beirão da Veiga, D. Cho, L. F. Pavarino, and S. Scacchi, *BDDC preconditioners for isogeometric analysis*, Math. Models Methods Appl. Sci., 23 (2013), pp. 1099–1142.

[7] L. Beirão da Veiga, D. Cho, L. F. Pavarino, and S. Scacchi, *Isogeometric Schwarz preconditioners for linear elasticity systems*, Comput. Methods Appl. Mech. Engrg., 253 (2013), pp. 439–454.

[8] L. Beirão da Veiga, D. Cho, and G. Sangalli, *Anisotropic NURBS approximation in isogeometric analysis*, Comput. Methods Appl. Mech. Engrg., 209–212 (2012), pp. 1–11.

[9] M. Bercovier and I. Soloveichik, *Additive Schwarz decomposition methods applied to isogeometric analysis*, submitted.

[10] S. C. Brenner and L.-Y. Sung, *BDDC and FETI-DP without matrices or vectors*, Comput. Methods Appl. Mech. Engrg., 196 (2007), pp. 1429–1435.

[11] N. Collier, L. Dalcin, D. Pardo, and V. M. Calo, *The cost of continuity: Performance of iterative solvers on isogeometric finite elements*, SIAM J. Sci. Comput., 35 (2013), pp. A767–A784.

[12] J. A. Cottrell, T. J. R. Hughes, and Y. Bazilevs, *Isogeometric Analysis. Towards Integration of CAD and FEA*, Wiley, New York, 2009.

[13] C. De Falco, A. Reali, and R. Vazquez, *GeoPDEs: A research tool for isogeometric analysis of PDEs*, Advan. Engrg. Softw., 42 (2011), pp. 1020–1034.

[14] M. Dryja, J. Galvis, and M. Sarkis, *BDDC methods for discontinuous Galerkin discretization of elliptic problems*, J. Complexity, 23 (2007), pp. 715–739.

[15] C. R. Dohrmann, *A preconditioner for substructuring based on constrained energy minimization*, SIAM J. Sci. Comput., 25 (2003), pp. 246–258.

[16] C. R. Dohrmann, *An approximate BDDC preconditioner*, Numer. Linear Algebra Appl., 14 (2007), pp. 149–168.

[17] C. R. Dohrmann and O. B. Widlund, *Some recent tools and a BDDC algorithm for 3D problems in H(curl)*, in Proceedings of the 20th International Conference on Domain Decomposition Methods (San Diego, CA, 2011), Lect. Notes Comput. Sci. Eng. 91, Springer, Berlin, 2013, pp. 15–26.

[18] C. Farhat, M. Lesoinne, P. LeTallec, K. Pierson, and D. Rixen, *FETI-DP: A dual-primal unified FETI method – part I. A faster alternative to the two-level FETI method*, Internat. J. Numer. Meth. Engrg., 50 (2001), pp. 1523–1544.

[19] K. Gahalaut, J. Kraus, and S. Tomar, *Multigrid methods for isogeometric discretization*, Comput. Methods Appl. Mech. Engrg., 253 (2013), pp. 413–425.

[20] C. Hesch and P. Betsch, *Isogeometric analysis and domain decomposition methods*, Comput. Methods Appl. Mech. Engrg., 213/216 (2012), pp. 104–112.

[21] T. J. R. Hughes, J. A. Cottrell, and Y. Bazilevs, *Isogeometric analysis: CAD, finite elements, NURBS, exact geometry, and mesh refinement*, Comput. Methods Appl. Mech. Engrg., 194 (2005), pp. 4135–4195.

[22] H. H. Kim, M. Dryja, and O. B. Widlund, *A BDDC method for mortar discretizations using a transformation of basis*, SIAM J. Numer. Anal., 47 (2008), pp. 136–157.

[23] H. H. Kim and X. Tu, *A three-level BDDC algorithm for mortar discretizations*, SIAM J. Numer. Anal., 47 (2009), pp. 1576–1600.

[24] S. K. Kleiss, C. Pechstein, B. Jüttler, and S. Tomar, *IETI - Isogeometric tearing and interconnecting*, Comput. Methods Appl. Mech. Engrg., 247/248 (2012), pp. 201–215.

[25] A. Klawonn and O. B. Widlund, *Dual-primal FETI methods for linear elasticity*, Comm. Pure Appl. Math., 59 (2006), pp. 1523–1572.

[26] J. H. Lee, *Domain Decomposition Methods for Reissner-Mindlin Plates Discretized with the Falk-Tu Elements*, Ph.D. Thesis, TR2011-937, Courant Institute, New York University, New York, NY, 2011.

[27] J. H. Lee, *Balancing Domain Decomposition by Constraints for Numerically Thin Reissner-Mindlin Plates Approximated by Falk–Tu Elements*, TR2013-958, Courant Institute, New York University, New York, NY, 2013.

[28] J. Li and O. B. Widlund, *FETI-DP, BDDC, and block Cholesky methods*, Internat. J. Numer. Methods Engrg., 66 (2006), pp. 250–271.

[29] J. Li and O. B. Widlund, *On the use of inexact subdomain solvers for BDDC algorithms*, Comput. Methods Appl. Mech. Engrg., 196 (2007), pp. 1415–1428.

[30] J. Li and X. Tu, *Convergence analysis of a balancing domain decomposition method for solving a class of indefinite linear systems*, Numer. Linear Algebra Appl., 16 (2009), pp. 745–773.

[31] J. Mandel and C. R. Dohrmann, *Convergence of a balancing domain decomposition by constraints and energy minimization*, Numer. Linear Algebra Appl., 10 (2003), pp. 639–659.

[32] J. MANDEL, C. R. DOHRMANN, AND R. TEZAUR, *An algebraic theory for primal and dual substructuring methods by constraints*, Appl. Numer. Math., 54 (2005), pp. 167–193.

[33] J. MANDEL, B. SOUSEDÍK, AND C. R. DOHRMANN, *Multispace and multilevel BDDC*, Computing, 83 (2008), pp. 55–85.

[34] D.-S. OH, O. B. WIDLUND, AND C. R. DOHRMANN, *A BDDC algorithm for Raviart-Thomas vector fields*, TR2013-951, Courant Institute, New York University, New York, NY, 2013.

[35] L. F. PAVARINO, O. B. WIDLUND, AND S. ZAMPINI, *BDDC preconditioners for spectral element discretizations of almost incompressible elasticity in three dimensions*, SIAM J. Sci. Comput., 32 (2010), pp. 3604–3626.

[36] A. TOSELLI AND O. B. WIDLUND, *Domain Decomposition Methods: Algorithms and Theory*, Comput. Math. 34, Springer-Verlag, Berlin, 2004.

[37] X. TU, *Three-level BDDC in three dimensions*, SIAM J. Sci. Comput., 29 (2007), pp. 1759–1780.

[38] X. TU AND J. LI, *A balancing domain decomposition method by constraints for advection-diffusion problems*, Commun. Appl. Math. Comput. Sci., 3 (2008), pp. 25–60.

[39] O. B. WIDLUND, *Iterative substructuring methods: Algorithms and theory for elliptic problems in the plane*, in Proceedings of the 1st International Symposium on Domain Decomposition Methods for Partial Differential Equations, R. Glowinski et al., eds., SIAM, Philadelphia, 1988, pp. 113–128.